Nonlinear Optical (NLO) Polymers. 3. NLO Polyimide with Dipole Moments Aligned Transverse to the Imide Linkage

Naoto Tsutsumi,* Mikio Morishima, and Wataru Sakai

Department of Polymer Science & Engineering, Kyoto Institute of Technology, Matsugasaki, Sakyo, Kyoto 606-8585, Japan

Received March 4, 1998; Revised Manuscript Received August 10, 1998

ABSTRACT: This paper presents a new class of nonlinear optical (NLO) polyimide for second harmonic generation (SHG). This new class of NLO polyimide consists of 2,4-diamino-4′-nitroazobenzene (2R-DIAMINE) with 3,3′4,4′-benzophenonetetracarboxylic dianhydride, in which the NLO dipole moment is aligned transverse to the main chain. 2R-DIAMINE was prepared from *m*-phenylenediamine with *p*-nitroaniline. The time dependence of the decay was found to be well-fitted by a Kohlrausch−Williams−Watts stretched exponential function. The difference of the orientational relaxation among the samples with different glass transition temperatures can be compared using the scaling relation of $\tau = A' \exp[(T_0 - T)/T]$ in which τ is the relaxation time and T_0 is the effective transition temperature for SHG activity. T_0 is in good agreement with the corresponding glass transition temperature. Enhanced orientational stability of the aligned NLO chromophore is ascribed to the rigid structure of the polyimide backbone. For the orientational relaxation at 100 °C, a relaxation time of over 50 years could be estimated, and a relaxation time of 3.8 years could be obtained at a higher temperature of 150 °C.

Introduction

Nonlinear optical (NLO) properties of polymeric materials have attracted extensive attention because of their potential applications to frequency doubling for data storage, electrooptic modulation for optical telecommunication and optical interconnects, and integrated optics.

For practical applications, long-term chemical and orientational stabilities of polymeric NLO materials are required at the operating temperatures which may vary between 80 and 125 °C depending on the configuration and application.[1,2] When polymeric NLO materials are fabricated as electrooptic devices, they may also be exposed to temperatures of ca. 200−250 °C for a short period of time.[1,2] As a minimum requirement, the orientational stability of aligned NLO chromophores at 80−125 °C for long periods of time is required. Several strategies have been suggested to achieve this goal. One approach is the use of the extensive cross-linking or network formation in NLO polymeric materials which suppresses the reorientation of the NLO chromophores.[3−7] Another approach is the utilization of high glass transition temperature (T_g) polymers, such as polyimides.[8−10]

Recently, we have synthesized a new type of polymer whose NLO chromophore is aligned transverse to the main chain: part of the NLO moiety is embedded in the polymer main chain, and its dipole moment extends transverse to the backbone.[11−13]

In this paper, we present the synthesis and the measure of second-order optical nonlinearity of the new NLO polyimide whose dipole moment aligns transverse to the polyimide backbone. The orientational stability of aligned NLO chromophores which generate the second harmonic (SH) light is discussed in relation to the rigid structure of the polyimide backbone.

Experimental Section

Monomers. 2,4-Diamino-4′-nitroazobenzene (2R-DIAMINE) was selected as the NLO chromophore. 2R-DIAMINE was synthesized via the one-step diazonium coupling reaction of *p*-nitrobenzene diazonium chloride with *m*-phenylenediamine as shown in Scheme 1. A solution of sodium nitrite (1.41 g, 0.0205 mol) in 3.0 mL of water was added dropwise with stirring to a cooled solution of *p*-nitroaniline (2.88 g, 0.0208 mol) dissolved in 5.25 mL of 35% hydrochloric acid and 20.0 mL of water at a temperature between 0 and 5 °C for 15 min. The diazonium salt obtained was coupled with *m*-phenylenediamine (2.18 g, 0.0202 mol) dissolved in 1.80 mL of 35% hydrochloric acid and 15.0 mL of water at a temperature between 0 and 5 °C over 30 min. Then sodium acetate (2.30 g, 0.028 mol) was added, the solution was left in an ice bath for 1 h, additional sodium acetate (2.30 g, 0.028 mol) was added, and the reaction mixture was left for 0.5 h. After the temperature was raised to room temperature, a 20% sodium hydroxide solution was added until the pH of solution reached 7 and the mixture was stirred at room temperature for 1 h. The resultant 2R-DIAMINE monomer was washed with water and recrystallized from ethanol. Figure 1 shows the ^{1}H NMR spectrum of 2R-DIAMINE measured in acetone-d_6 at 20 °C. Elemental analysis gives the following composition: C, 55.76; H, 4.31; O, 26.54; N, 13.12. This is compared with the calculated values: C, 56.03; H, 4.31; O, 27.22; N, 12.44. 3,3′,4,4′-Benzophenonetetracarboxylic dianhydride (W) was used as received.

Scheme 1

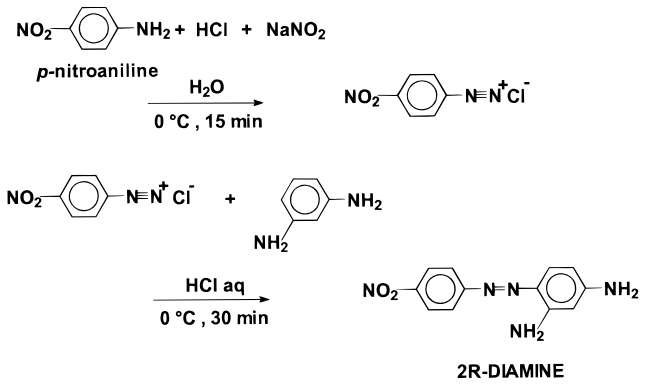

Preparation of Poly(amic acid) and Film Processing. The synthetic scheme of polyimide (2RW) is shown in Scheme

* To whom all correspondence should be addressed.

10.1021/ma9803436 CCC: $15.00
Published on Web 10/17/1998

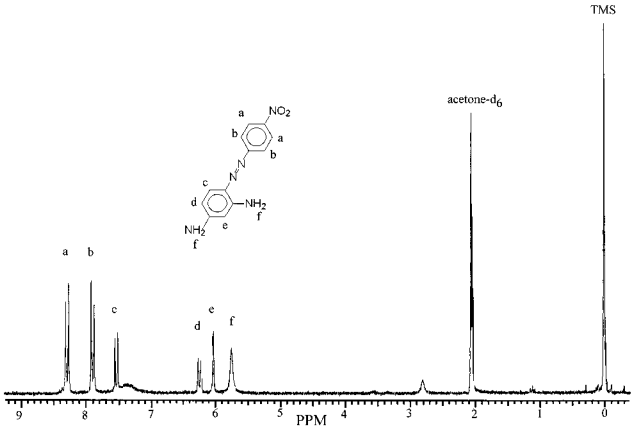

Figure 1. ^{1}H NMR spectrum of 2R-DIAMINE measured in acetone-d_6 at 20 °C.

2. 2R-DIAMINE (0.50 g, 1.95 mmol) was reacted with W (0.63 g, 1.95 mmol) in distilled *N*-methyl-2-pyrrolidone (NMP) first at a temperature between 0 and 5 °C for 4 h and then at room temperature for 15 h to prepare a poly(amic acid) solution. Poly(amic acid) films were cast on an indium tin oxide (ITO) coated glass substrate from the poly(amic acid) solution diluted by distilled NMP. After the cast films were dried at 45 °C for 12 h, they were subjected to concurrent in situ poling and imidization. The polyimide films (2RW) had thicknesses ranging between 2 and 6 μm.

In Situ Poling and Simultaneous Imidization. A two-step corona poling process was employed to orient the NLO chromophore. The distance between tungsten wire used for corona poling and the sample was 1.4 cm. The diameter of tungsten wire is 0.1 ∅. In the first poling process, the sample was heated to a given temperature between 140 and 200 °C at a heating rate of 10 °C/min and successively held at those temperatures for 1 h, while high voltage between 5.0 and 7.0 kV was applied to a corona wire. In the second poling process, the temperature was increased to a temperature between 200 and 260 °C at a heating rate of 10 °C/min and held at this temperature for 30 min in the corona field. Finally the sample was cooled to room temperature in the presence of the poling field. Appropriate first and second poling temperatures are reported in the Results and Discussion section.

SHG Measurements. The Maker fringe method[14,15] was employed to measure the SH intensity in the poled films. The laser source was a Continuum model Surelite-10 Q-switched Nd:YAG pulse laser with a 1064-nm p-polarized fundamental beam (320-mJ maximum energy, 7-ns pulse width, and 10-Hz repeating rate). The SH wave generated in the film was detected by a photomultiplier. The SH signal was averaged in a gated integrator and boxcar averager module and transferred to a microcomputer through an interface module. The experimental procedure is described in refs 16 and 17.

Characterization. Ultraviolet−visible spectra of the films were measured on a Shimadzu model UV-2101PC spectrophotometer. The m-line method using a prism coupling apparatus was employed to measure the refractive indices of the films. The laser sources were a polarized He−Ne laser (632.8 nm) and a laser diode (830 nm). The prism was a TaFD21 (HOYA glass) with a high refractive index (1.92588 at 632.8 nm), to which the spin-coated or cast film was coupled via an air gap. Guided-wave spectra (m lines) were recorded and the refractive indices calculated. Nuclear magnetic resonances (NMR) were measured using TMS as an internal standard at 20 °C using a Varian model Gemini-200. Differential scanning calorimetry (DSC) was carried out at a heating rate of 10 °C/min in a nitrogen atmosphere, using a Perkin-Elmer DSC7 instrument controlled by a 1020 TA workstation. Thermogravimetric analysis (TGA) was performed with a Shimadzu model DT-30 thermogravimetric analyzer at a heating rate of 10 °C/min in a nitrogen atmosphere.

Results and Discussion

Polymer Structure. Polyimide films (2RW) were prepared by casting the poly(amic acid) solutions. Thermal imidization is affected first by heating the sample to 160 °C with simultaneous poling and finally by heating it to 200, 230, and 260 °C with simultaneous poling. Figure 2 shows the UV−vis absorption spectra for the 2RW polyimide, 2R-DIAMINE and a polyamide-prepared from 2R-DIAMINE and sebacic acid (2R10). The spectrum of 2R-DIAMINE was measured in an ethanol solution, and the other two spectra were measured on films. Absorption maxima λ_{max} are 500 nm for 2R-DIAMINE, 420 nm for 2R10, and 350 nm for 2RW. Significant blue shift of λ_{max} in 2RW is ascribed to the reduced electron-donating ability of amino groups upon conversion to the imides; the strongest electron donating substituent is the amino group (−NH_2), followed by the amide group (−NHCO-), and finally the imide group (−$N(CO)_2$−). Figure 3 shows the DSC thermogram for 2RW imidized at various temperatures ranging between 200 and 260 °C. Increasing the final imidization temperature leads to an increase of the glass transition temperature (T_g). The difference between the measurement temperature and T_g is related to the orientational stability of aligned NLO chromophores in the poled polymer films (vide infra).

Refractive Indices. The refractive indices (RI) for the transverse electric field (TE) mode are measured using the m-line method at wavelengths of 632.8 and 830 nm. The RI values for the unpoled 2RW film at these wavelengths are listed in Table 1. The wavelength dispersion of the RI, $n_f(\lambda)$, can be fitted to a one-oscillator Sellmeier-dispersion formula

$$n_f^2(\lambda) - 1 = \frac{q}{1/\lambda_0^2 - 1/\lambda^2} + A \qquad (1)$$

where λ_0 is the absorption wavelength of the dominant oscillator, q is a measure of the oscillator strength, and A is a constant containing the sum of all of the other oscillators. Figure 4 shows the RI data at 632.8 and 830 nm and the predicted curve of the RI wavelength dispersion calculated from eq 1 with $\lambda_0 = 350$ nm. The RI values at 532 and 1064 nm obtained from the calculated curve, which are also listed in Table 1, are used for the calculation of SH coefficients.

Optimum Poling Conditions for SHG. The SH coefficients for 2RW are measured relative to a Y-cut quartz plate ($d_{11} = 1.2 \times 10^{-9}$ esu (0.5 pm/V)). Typical Maker fringe patterns were observed for both p-polarized and s-polarized fundamental beams. These are shown for the samples poled at 6.0 kV at 160 °C for 1 h and finally at 200 °C for 30 min in Figure 5. It is important to optimize the poling condition (poling voltage, temperature, and time) to obtain a maximum SH signal. The poling time was fixed for 1 h because the SH coefficient was leveled out at the time above 1 h. The SH coefficient increases with the applied voltage up to a point but decreases slightly above 6 kV as shown in Figure 6 a. As shown in Figure 6b, the initial poling temperature of 160 °C produces the maximum d_{33} value. The final poling temperature was fixed at 200 °C for 30 min. Optimum poling conditions were 6.0-kV poling voltage with an initial temperature of 160 °C and a final poling temperature of 200 °C.

Thermal Stability of SHG Activity. Figure 7 shows the long-term thermal stability of d_{33} when the

Scheme 2

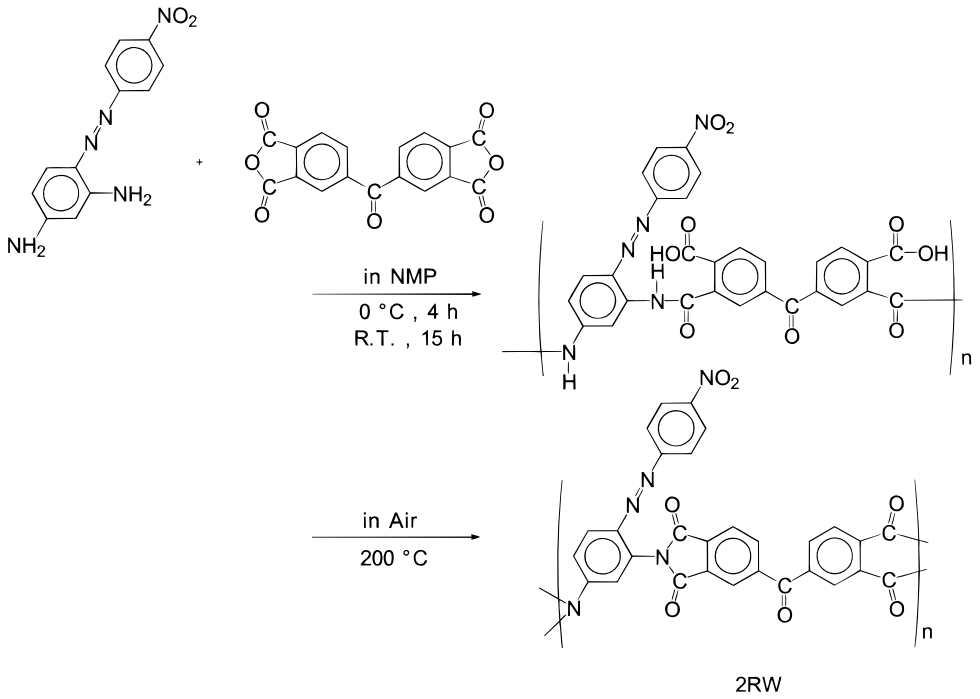

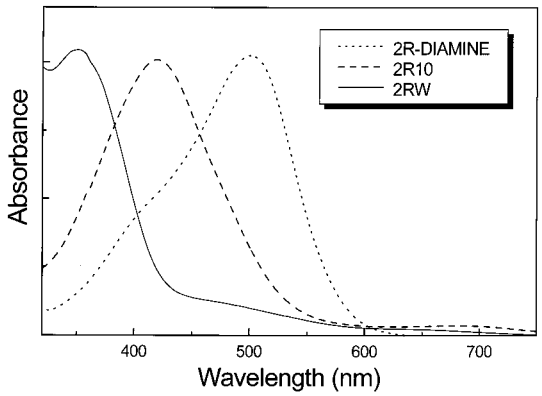

Figure 2. UV−vis absorption spectra for 2RW polyimide, 2R-DIAMINE, and 2R10 polyamide.

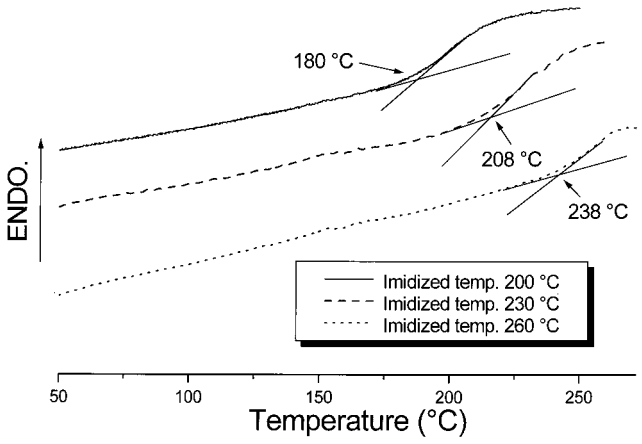

Figure 3. DSC thermograms for the samples imidized at different temperatures of 200, 230, and 260 °C.

film is heated to 100 (a) and 150 °C (b). The plot in the figure is the normalized second harmonic coefficient d_{33}. The polymer 2RW has excellent long-term orientational stability at 100 °C after a small activity loss within a few hours after poling. The orientational stability of 2RW is also good at 150 °C.

Table 1. Refractive Indices for Samples Measured at 632.8 and 830 nm and Predicted Values at 532 and 1064 nm Using the Sellmeier Equation with $\lambda_0 = 350$ nm

	wavelength(nm)			
sample	632.8	830	532	1064
2RW	1.7157	1.6980	1.7408	1.6905

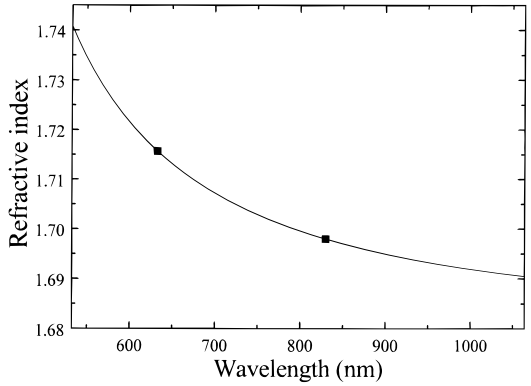

Figure 4. Plot of RI at wavelengths of 632.8 and 830 nm and the predicted curve (solid curve) of the RI wavelength dispersion calculated from eq 1 with $\lambda_0 = 350$ nm.

The time-dependent decay of SHG activity can be expressed by either a Kohlrausch−Williams−Watts (KWW) stretched exponential form or a sum of two exponential fits. Both expressions are often used to characterize the orientational relaxation of NLO dipoles in polymeric matrices. As pointed out in our previous report,[13] the time-dependent decay curves are fitted well by either form; however, the sum of two exponentials requires three fitting parameters instead of two for a KWW stretched exponential fit. A physical model involving two distinct exponents for the shorter and longer time constants leads to complexities for characterizing the molecular motion of NLO chromophores in amorphous polymer matrices. In the present case, a

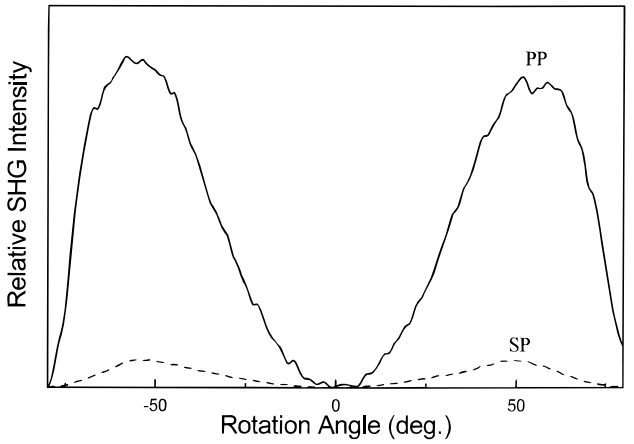

Figure 5. Typical Maker fringe pattern of sample film poled at 6.0 kV at 160 °C for 1 h and finally at 200 °C for 30 min.

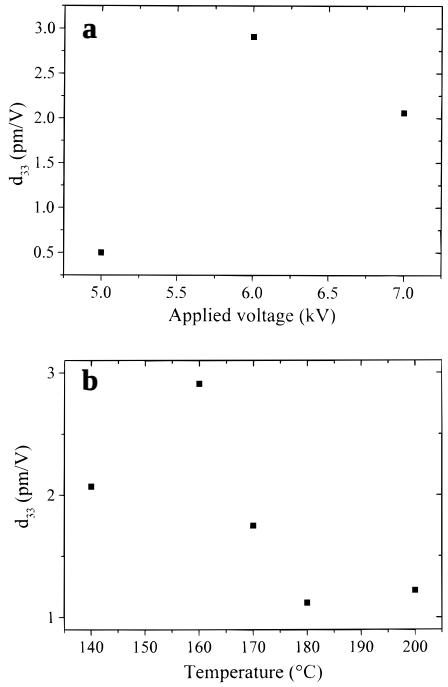

Figure 6. Poling condition of 2RW: (a) Change of d_{33} values when the corona voltage is varied from 5 to 7 kV. The initial and final poling temperatures are 160 and 200 °C, respectively. (b) Change of d_{33} values when the initial poling temperature is varied from 140 to 200 °C.

KWW stretched exponential fit is employed to characterize the relaxation of the aligned NLO chromophores in 2RW:

$$d = d_0 \exp(-(t/\tau)^{\beta}) \quad (0 < \beta \leq 1) \qquad (2)$$

where τ is the characteristic relaxation time and β is a measure of width of the distribution of relaxation times and the extent of deviation from a single-exponential behavior. When $\beta = 1$, the time-dependent decay corresponds to a single-exponential decay profile. The characteristic relaxation time τ is the time required for the system to decay to 1/e of its initial value. The solid curve in Figure 7 is the fitted curve using the KWW stretched exponential form. Each time-dependent decay curve can be fitted well by the KWW stretched exponential curves with appropriate relaxation time τ and β values as fitting parameters for each temperatures. Table 2 summarizes the obtained τ and β values for both

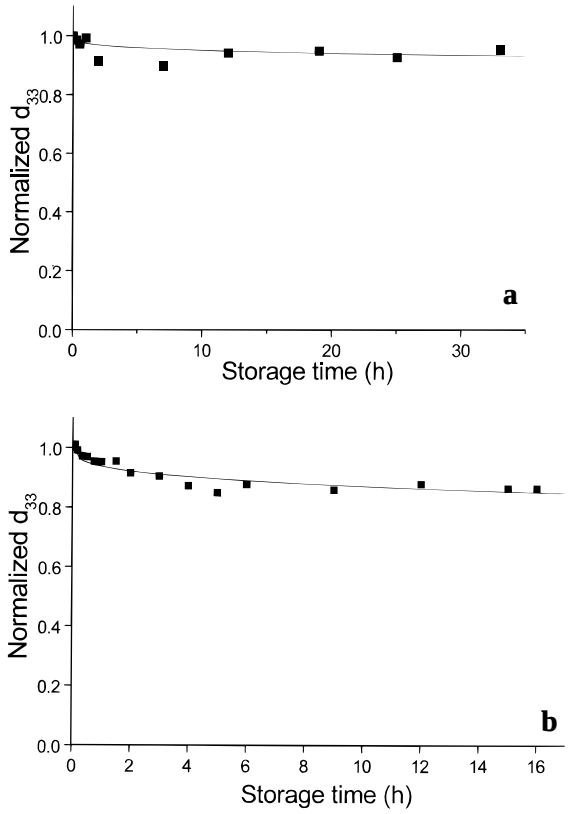

Figure 7. Long-term thermal stability of d_{33} values when sample film is stored at 100 (a) and 150 °C (b).

Table 2. Relaxation Time τ (s) and β Values for Samples Obtained from the Appropriate Fitting of the KWW Stretched Exponential Function

	holding temperature (°C)	
	100	150
τ value (s)	1.67×10^9	9.3×10^6
β value	0.28	0.33

temperatures. It is noted that the characteristic relaxation time for 2RW at 100 °C is 1.67×10^9 s (=52.9 year) and this relaxation time is enough for most practical operations.

Effect of Final Poling Temperature on SHG Activity. Figure 8 shows the dynamic thermal profiles of d_{33} vs annealing temperature for 2RW films with final poling temperatures of 200 and 230 °C. The plots in the figure are normalized d_{33} values. The effective transition temperatures, T_0, representing an onset decay temperature are 174 and 200 °C for the samples poled at 200 and 230 °C, respectively. T_0 definitely increases with increasing final poling temperature. This means that the orientational stability of the aligned NLO chromophore is significantly enhanced by the increase in the final poling temperature. This enhancement is reflected by the observed difference in the reorientational relaxation times of samples held at a fixed temperature of 150 °C as listed in Table 3. This enhancement of the orientational stability of the aligned NLO chromophore is apparently related to the degree of the imidization. The degree of imidization can be estimated from the glass transition temperatures, T_g, determined by DSC as shown in Figure 3. Higher poling (annealing) temperatures lead to higher glass transition temperatures, i.e., more imidization. As

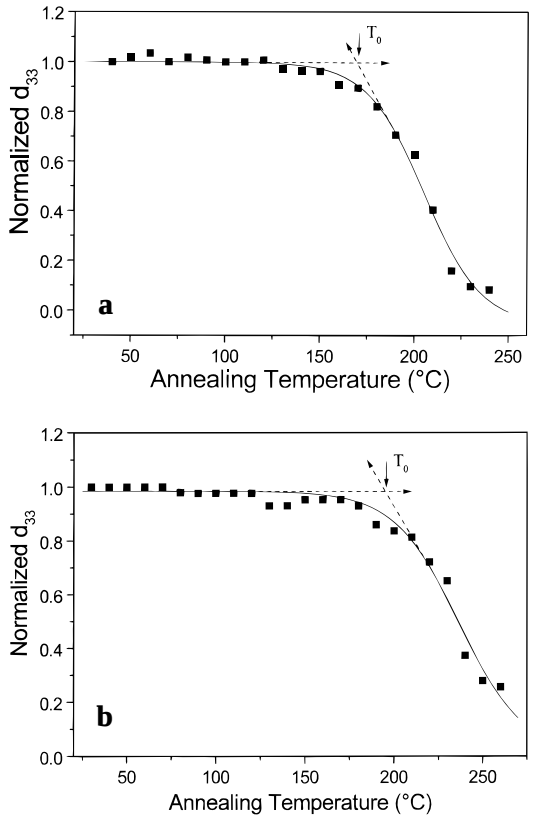

Figure 8. Dependence of d_{33} on the annealing temperature for the sample poled at 200 (a) and 230 °C (b).

Table 3. Relaxation Time τ and β Value for 2RW with Different Final Poling Temperatures (Holding Temperature Is 150 °C)

	final poling temperature (°C)			
	200	220	230	260
τ value (s)	9.3×10^6	2.1×10^7	3.9×10^7	1.2×10^8
β value	0.33	0.27	0.26	0.28

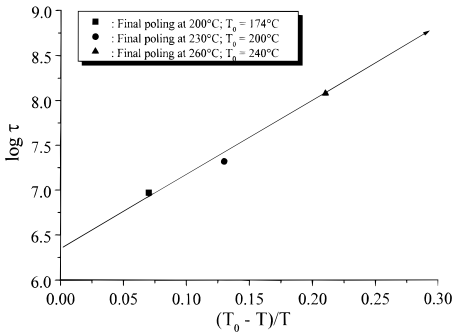

Figure 9. Scaling plot of logarithmic τ vs $(T - T_0)/T$.

described in our previous paper,[13] the scaling relationship[2,8] of

$$\tau(T) = A' \exp\left(\frac{T_0 - T}{T}\right) \tag{3}$$

is proposed, where A' is a constant and T_0 is the effective transition temperature for SHG activity. This relationship may be used to predict the orientational relaxation of NLO moieties in polymers with different transition temperatures. Figure 9 shows the scaling plot of the relaxation times in the present system calculated from eq 3 with T_0 = 174, 200, and 240 °C for the samples

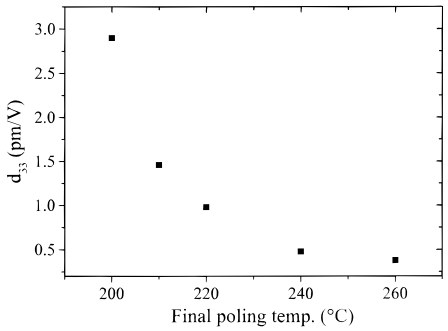

Figure 10. Dependence of d_{33} on the final poling temperature. The final poling time is fixed at 30 min. The initial poling temperature and time are 160 °C and 1 h, respectively. The poling field is 6.0 kV.

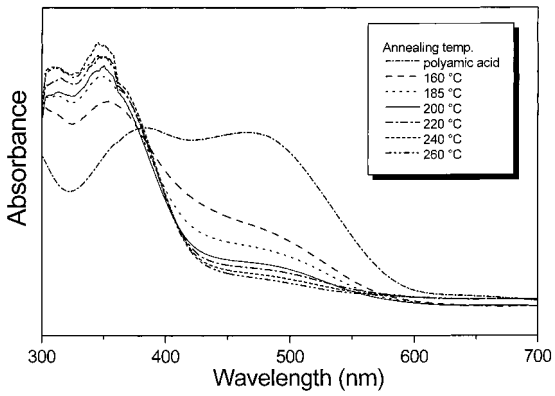

Figure 11. Changes of UV−vis absorption spectra when the annealing temperature is varied.

with final poling temperatures of 200, 230, and 260 °C, respectively. These T_0's should be closely related to the glass transition temperature T_g of the polymers. Indeed, T_0's are in good agreement with the corresponding T_g values listed in Figure 3.

The d_{33} value decreases with an increase of the final poling temperature. This behavior is shown in Figure 10. The changes of the UV−vis absorption spectra are shown upon annealing at higher temperature in Figure 11. It is clear that the absorption around 500 nm is decreased and that at 350 nm is increased with an increase in the annealing temperature. These changes in the absorption spectra suggest that the apparent hyperpolarizability of the NLO chromophore in polyimide is decreased. As described above, the electron-donating ability of the imide linkage is weaker, which leads to a lower hyperpolarizability of the azobenzene NLO chromophore. Thermogravimetric results show that no weight loss was measured up to 300 °C. Therefore, it is not likely that the depression of SHG activities is based on the decomposition of the NLO chromophore due to the exposure to higher temperatures.

Conclusion

The combination of the imide linkage and the NLO chromophore whose dipole moment aligns transversely to the backbone gave rise to a new type of NLO polyimide. Orientational relaxation of the NLO chromophore was investigated for the sample poled at different final temperatures. The time dependence of the decay was found to be well represented by a KWW stretched exponential function. The difference of the orientational relaxation among the samples with different glass transition temperatures can be compared

using the scaling relation. Enhanced orientational stability of the aligned NLO chromophore is ascribed to the rigid structure of the polyimide backbone. Larger degrees of imidization cause the more enhanced orientational stability of the aligned NLO chromophore, but simultaneously the NLO activity is dramatically reduced with increasing imidization. Further study, for example, the introduction of an electron-donating group in the NLO moiety, should be considered to overcome this conflict of interest.

Acknowledgment. This work is, in part, supported by Grants-in-Aid for Scientific Research on Priority Areas (No. 08236223 and 09222214) from the Ministry of Education, Science, Culture and Sports, Japan.

References and Notes

(1) Stähelin, M.; Burland, D. M.; Ebert, M.; Miller, R. D.; Smith, B. A.; Twieg, R. J.; Volksen, W.; Walsh, C. A. *Appl. Phys. Lett.* **1992**, *61*, 1626.
(2) Weder, C.; Neuenschwander, P.; Suter, U. W.; Prêtre, P.; Kaatz, P.; Günter, P. *Macromolecules* **1995**, *28*, 2377.
(3) Jungbauer, D.; Reck, B.; Twieg, R.; Yoon, D. Y.; Willson, C. G.; Swalen, J. D. *Appl. Phys. Lett.* **1990**, *56*, 2610.
(4) Ranon, P. M.; Shi, Y.; Steier, W. H.; Xu, C.; Wu, B.; Dalton, L. R. *Appl. Phys. Lett.* **1993**, *62*, 2605.
(5) Boogers, J. A. F.; Klaase, P. Th. A.; de Vliger, J. J.; Tinnemans, A. A. *Macromolecules* **1994**, *27*, 205.
(6) White, K. M.; Francis, C. V.; Isackson, A. J. *Macromolecules* **1994**, *27*, 3619.
(7) Tsutsumi, N.; Yoshizaki, S.; Sakai, W.; Kiyotsukuri, T. *Macromolecules* **1995**, *28*, 6437.
(8) Prêtre, P.; Kaats, P.; Bohren, A.; Günter, P.; Zysset, B.; Ahlheim, M.; Stähelin M.; Lehr, F. *Macromolecules* **1994**, *27*, 5476.
(9) Miller, R. D.; Burland, D. M.; Jurich, M.; Lee, V. Y.; Moylan, C. R.; Thackara, J. I.; Twieg, R. J.; Verbiest, T.; Volksen, W. *Macromolecules* **1995**, *28*, 4970.
(10) Miller, R. D.; et al. in *Photonic and Optoelectronic Polymers*; Jenekhe, S. A., Wynne, K. J., Eds.; ACS Symposium Series 672; American Chemical Society: Washington, DC, 1997; pp 100−122.
(11) Tsutsumi, N.; Matsumoto, O.; Sakai, W.; Kiyotsukuri, T. *Appl. Phys. Lett.* **1995**, *67*, 2272.
(12) Tsutsumi, N.; Matsumoto, O.; Sakai, W.; Kiyotsukuri, T. *Macromolecules* **1996**, *29*, 592.
(13) Tsutsumi, N.; Matsumoto, O.; Sakai, W. *Macromolecules* **1997**, *30*, 4584.
(14) Maker, P. D.; Terhune R. W.; Nisenoff, M.; Savage, C. M. *Phys. Rev. Lett.* **1962**, *8*, 21.
(15) Jerphagnon, J.; Kurtz, S. K. *J. Appl. Phys.* **1970**, *40*, 1667.
(16) Tsutsumi, N.; Ono, T.; Kiyotsukuri, T. *Macromolecules* **1993**, *26*, 5447.
(17) Tsutsumi, N.; Fujii, I.; Ueda, Y.; Kiyotsukuri, T. *Macromolecules* **1995**, *28*, 950.

MA9803436